Optimization of a Redundant Serial Spherical Mechanism for Robotic Minimally Invasive Surgery

C. A. Nelson[1], M. A. Laribi[2], and S. Zeghloul[3]

[1] *Department of Mechanical and Materials Engineering, University of Nebraska-Lincoln, Lincoln, NE 68588-0526, USA, e-mail: cnelson5@unl.edu*

[2] *Dept. of GMSC, Pprime Institute, CNRS - University of Poitiers - ENSMA - UPR 3346, France, e-mail: med.amine.laribi@univ-poitiers.fr*

[3] *Dept. of GMSC, Pprime Institute, CNRS - University of Poitiers - ENSMA - UPR 3346, France, e-mail: said.zeghloul@univ-poitiers.fr*

Abstract. Serial spherical linkages have been used in the design of a number of robots for minimally invasive surgery, in order to mechanically constrain the surgical instrument with respect to the incision. However, the typical serial spherical mechanism suffers from conflicting design objectives, resulting in an unsuitable compromise between avoiding collision with the patient and producing good kinematic and workspace characteristics. In this paper we propose a redundant serial spherical linkage to achieve this purpose and present a multi-objective optimization for achieving the aforementioned design goals. The sensitivity of the solution to uncertainties in the design parameters is investigated.

Key words: serial spherical mechanism, redundant linkage, surgical robot, minimally invasive surgery.

1 Introduction

In minimally invasive surgery, the instruments are inserted through small incisions, which thereafter serve as kinematic constraints allowing four degrees of freedom (DOF) per instrument (three rotations centered at the incision point, often referred to as the remote center of motion [3], and one translation through the incision) [18]. Various spherical mechanisms have been proposed in the surgical robotics literature for mechanically constraining the instruments to avoid motions that would cause trauma to the tissue at the incision location [1, 5, 6, 11, 14, 15]. Among these are serial spherical linkages, either actuated at each joint [2, 16] or powered by actuators on a fixed base with motion transmitted through gearing [17, 18], cables [7], or other means.

The typical serial spherical mechanism has three intersecting rotation axes fixed in two links, providing the three rotational DOF mentioned previously. The lengths of the two links must be chosen carefully in order to provide adequate workspace (usually considered as a cone whose apex half-angle is at least 30 degrees [12]) without interference (collision) between the robot and the patient. However, these two primary design objectives are in opposition, as the larger links required to increase workspace also increase the impingement of the robot in the space occupied by the patient.

In this paper, we propose solving this problem by introducing an additional (redundant) link. We present a multi-objective optimization considering the workspace requirements, the kinematic performance, and the collision constraint.

2 Methods

The proposed robot architecture is a classic serial spherical linkage (two links and three joints with intersecting axes) with a redundant link (and joint) added, as shown in Fig. 1. Singularities (well know for this type of robot) are avoided by restricting the motion of each joint to avoid alignment of adjacent links. We similarly avoid internal collisions within the robot itself. Thus the robot remains in a single operating mode throughout its used workspace. The problem consists of finding the optimal link parameters, expressed as angles α_i, which satisfy the objectives and constraints mentioned previously.

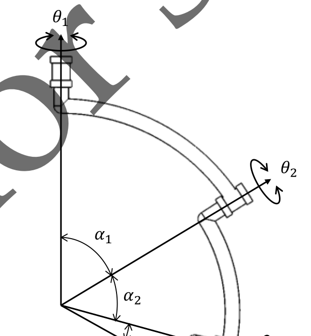

Fig. 1 Redundant serial spherical arm

The task-based synthesis and optimization of medical robots is a rich topic area in the literature [3, 8]. Building from classical performance indices in robotics, specialized indices have been proposed to account for workspace requirements in this type of robot [9, 17]. However, it is less common to see optimization approaches in medical robotics which account for the avoidance of collisions between the robot and the patient.

We adopt a multi-objective optimization approach considering workspace, kinematic performance, and robot compactness as criteria. For the workspace criterion, we recognize that the actual workspace will not be exactly equal to the conical section of a spherical surface described previously, so we base the optimization on a conservative measure of such an idealized workspace inscribed within the actual workspace. The actual workspace is directly calculated by forward kinematics, discretizing the joint space within the limited range of motion previously mentioned. Collision avoidance is directly accounted for within the optimization subroutine by throwing out any workspace points at which any part of the robot penetrates a planar boundary passing through the surgical incision and orthogonal to the neutral axis of the surgical trocar. Such cases are shown in Fig. 2. For the kinematic performance criterion, we use the improved indices proposed by Olds [10], which give worst-case measures of position error (max) and velocity (min) in the two-dimensional workspace. Compactness is measured as the sum of the link angles α_i.

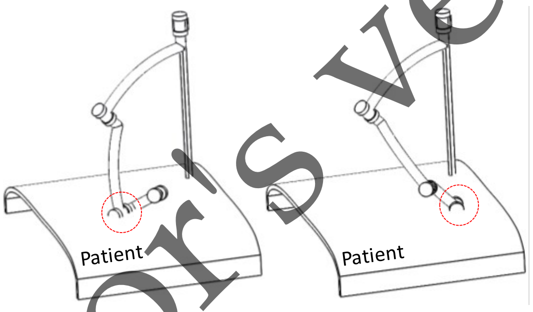

Fig. 2 Robot/patient collision cases (circle indicates area of collision)

As inputs, we use the three joint angles ($\theta_{1,2,3}$), and as outputs the pan (left-to-right) and tilt (down-to-up) angles intuitive to surgeons in the context of laparoscopic camera orientation. The joint angle θ_4 is not used as an input since it is for instrument self-rotation and does not affect tool position. Based on a neutral position with all robot links aligned and extended in the positive tilt direction,

$$p = \alpha_1 \sin\theta_1 + \alpha_2 \sin(\theta_1 + \theta_2) + \alpha_3 \sin(\theta_1 + \theta_2 + \theta_3) \quad (1)$$

$$t = \alpha_1 \cos\theta_1 + \alpha_2 \cos(\theta_1 + \theta_2) + \alpha_3 \cos(\theta_1 + \theta_2 + \theta_3) \quad (2)$$

where p is the pan angle and t is the tilt angle, and the Jacobian is

$$\mathbf{J} = \begin{bmatrix} J_{11} & J_{12} & J_{13} \\ J_{21} & J_{22} & J_{23} \end{bmatrix} \quad (3)$$

$$J_{11} = \alpha_1 cos\theta_1 + \alpha_2 cos(\theta_1 + \theta_2) + \alpha_3 cos(\theta_1 + \theta_2 + \theta_3)$$

$$J_{12} = \alpha_2 cos(\theta_1 + \theta_2) + \alpha_3 cos(\theta_1 + \theta_2 + \theta_3)$$

$$J_{13} = \alpha_3 cos(\theta_1 + \theta_2 + \theta_3)$$

$$J_{21} = -\alpha_1 sin\theta_1 - \alpha_2 sin(\theta_1 + \theta_2) - \alpha_3 sin(\theta_1 + \theta_2 + \theta_3)$$
$$J_{22} = -\alpha_2 sin(\theta_1 + \theta_2) - \alpha_3 sin(\theta_1 + \theta_2 + \theta_3)$$
$$J_{23} = -\alpha_3 sin(\theta_1 + \theta_2 + \theta_3)$$

Because the robot is redundant, the Jacobian matrix is not square. Therefore, we adapt the indices [10] to include the pseudoinverse:

$$\mu_{\min} = \frac{1}{\max\|\mathbf{J}*_i\|_2} \tag{4}$$

$$\mu_{\max} = \max\frac{\|\mathbf{J}\dot{\boldsymbol{\theta}}\|_2}{\|\dot{\theta}\|_\infty} \tag{5}$$

with the pseudoinverse of the Jacobian expressed as

$$\mathbf{J}^* = \mathbf{J}^{\mathrm{T}}(\mathbf{J}\mathbf{J}^{\mathrm{T}})^{-1} \tag{6}$$

and $\mathbf{J}_i^*$ indicating the ith row of $\mathbf{J}^*$. Here $\mu_{\min}$ represents the worst-case velocity, and $\mu_{\max}$ represents the worst-case position error. As suggested in [10], we allow the velocity vector to take on its various possible extreme values in the calculation of $\mu_{\max}$:

$$\dot{\boldsymbol{\theta}} = \begin{Bmatrix}1\\1\\1\end{Bmatrix}, \begin{Bmatrix}1\\-1\\1\end{Bmatrix}, \begin{Bmatrix}1\\1\\-1\end{Bmatrix}, \begin{Bmatrix}1\\-1\\-1\end{Bmatrix} \tag{7}$$

The kinematic performance is expressed as the worst of these two metrics ($\mu_{\min}$ and $\mu_{\max}$) at each point in the workspace and averaged across the entire feasible workspace (as sampled in the joint space).

The *fgoalattain*() function in MATLAB was used to carry out the optimization. This function is an implementation of the sequential quadratic programming (SQP) method and allows multiple objectives to be weighted within a single objective function. In contrast to the Pareto approach, in which no criterion is allowed to get worse from one iteration to the next, the *fgoalattain*() function provides better convergence by allowing the search direction to experience "tradeoffs" between the individual criteria in order to optimize the global criterion.

The redundant serial arm was optimized using allowable ranges of the link parameters $\boldsymbol{\alpha}$ and joint variables $\boldsymbol{\theta}$ as indicated in Table 1, and weights of 0 on workspace and collision avoidance, 0.3 on kinematic performance, and 0.5 on compactness (where 0 indicates a hard constraint and 1 represents an unenforced objective). These weights were chosen to enforce the need for safety and adequate workspace without completely neglecting the other desirable characteristics.

Table 1. Parameter values used in optimization

Parameter	*Lower Bound (°)*	*Upper Bound (°)*
$\alpha_{1,2,3}$	9	120
θ_1	-85	85
θ_2	5	175
θ_3	-175	-5

3 Results and discussion

The serial arm parameters obtained through optimization were $S{:}\{\alpha_1 = 46.7°, \alpha_2 = 44°, \alpha_3 = 18.9°\}$. The resulting robot is shown in Fig. 3. The workspace and collision avoidance criteria are fully satisfied, and the kinematic performance of the robot can be seen in Fig. 4. As allowed by the *fgoalattain*() function, neither the performance nor the compactness criteria were fully satisfied; this is to be expected, as the robot is not expected to be perfectly small nor fully isotropic throughout the workspace.

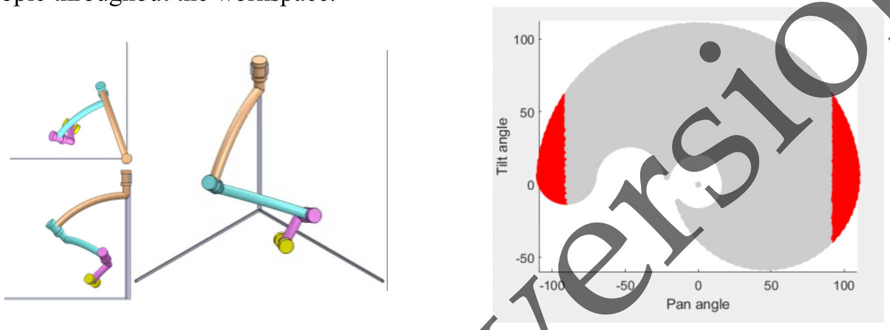

Fig. 3 The obtained redundant serial spherical mechanism: (left) computer rendering; (right) pan-tilt workspace – red area is excluded based on collision

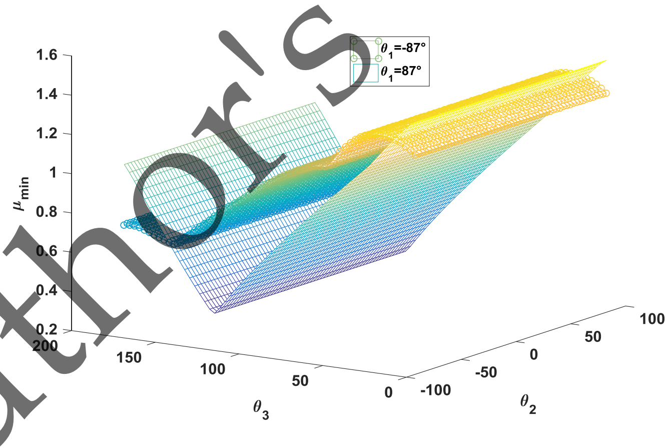

Fig. 4 Performance of optimized manipulator: the distribution of $\mu_{\min}$ in joint space for $\theta_1 = \pm 87°$.

The obtained result indicates that the algorithm performs in a stable manner and provides consistent results. Next, the variability of the optimized redundant serial spherical linkage performance generated by the design paramters will be estimated. Thus, the case of optimal solution S, given at the beigining of this section, will be studied.

Each uncertain design parameter is represented by a statistical distribution. For a normal distribution this requires a mean value and a standard deviation. A Monte Carlo simulation [13] is performed for every design parameter where each evaluation consists of a specified number of runs as shown in Fig. 5.

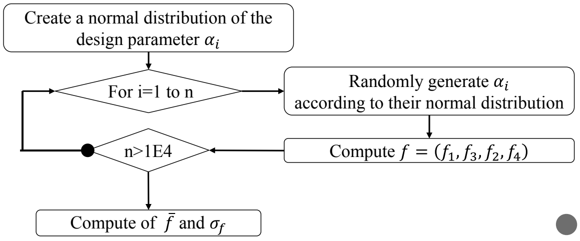

Fig. 5 Monte Carlo simulation flowchart

For each Monte Carlo simulation, all the deterministic design variables, α_i, are fixed at their nominal values and the uncertain design variables, $\tilde{\alpha}_i$, are selected randomly from their statistical distributions assumed to vary within ±5% of the specified nominal values. With the Monte Carlo simulation, we perform $n = 10^4$ simulations to determine the mean value $\bar{f} = \{\bar{f}_1, \bar{f}_2, \bar{f}_3, \bar{f}_4\}$ as well as the respective standard deviations $\sigma_f = \{\sigma_{f_1}, \sigma_{f_2}, \sigma_{f_3}, \sigma_{f_4}\}$. The evolution of each performance is presented in Fig. 6. The sensitivity study result of the optimal solution S is shown in Table 2.

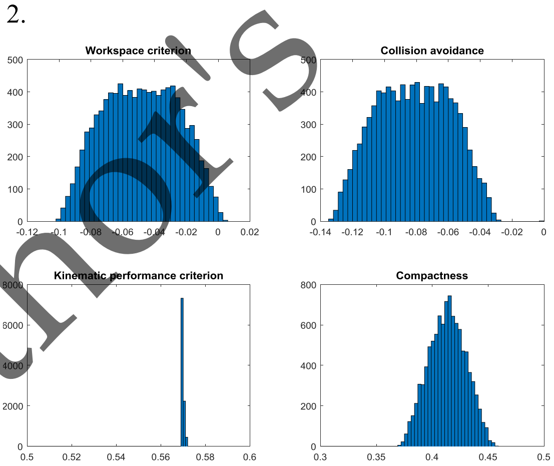

Fig. 6 Effect of the design parameters’ uncertainty on the objective functions

We observe through these data the high sensitivity of the structure on the first two criteria, respectively workspace and collision avoidance. The variation around the optimal values of the design parameters leads to a large violation of the performance criteria in relation with the workspace and collision avoidance. This first observation justifies the choice of the very strict condition on the respective weights at the definition of the optimization problem.

Table 2. Sensitivity of the optimal solution.

Objective function	*Mean value* $\bar{f_i}$	*Standard deviation* σ_{f_i}	*Sensitivity* s_i
Workspace: f_1	0.0483	0.0232	144.28%
Collision: f_2	0.0815	0.0232	85%
Kinematic performance: f_3	0.5697	0.0057	3%
Compactness: f_4	0.4133	0.0169	12%

In contrast, the last two criteria, respectively kinematic performance and compactness, are less sensitive to the disturbance of the design parameters. The calculated sensitivity is of about 15%.

Consequently, by considering the uncertainties of the design parameters the workspace and collision avaidance given by the optimal solution S are no longer guaranteed. These two performances should be defined as constraints and not as criteria.Therefore, the optimal solutions, obtained by the multi-objective optimization presented previously, are not robust due to the design parameter uncertainties. This problem merits further work.

6 Conclusions

In this work a redundant serial spherical linkage has been presented to cope with the problems of the classic serial spherical mechanism for medical robots. Four design objectives have been presented and adapted to the proposed redundant mechanism: workspace, kinematic performance, avoiding collision and compactness. A multi-objective optimization problem is formulated in this aim and solved using the *fgoalattain*() function. The obtained optimal solution perfectly satisfies the workspace criterion as well as the collision avoidance requirement. However, neither the performance nor the compactness criteria were fully satisfied and this is due to the tradeoffs allowed by the optimization method. This type of result facilitates the designer’s choice of a suitable solution by generating a specific solution without going through a Pareto front. A sensitivity study is performed based on the Monte Carlo method which shows that the deterministic optimal solutions can be strongly affected by the uncertainties in the design parameters. A robust multi-objective optimization will be addressed in future work to cope with this sensitivity problem.

Acknowledgments This work is sponsored by the French government research program Investissements d'avenir through the Robotex Equipment of Excellence (ANR-10-EQPX-44) and by a faculty development fellowship from the University of Nebraska-Lincoln.

References

1. Berkelman, P., Boidard, E., Cinquin, E., and Troccaz, J.: LER : The Light Endoscope Robot. In Proc. IEEE/RSJ Int. Conf. on Intelligent Robots and Systems (IROS), pp. 2835-2840, Las Vegas, NV, USA (2003)
2. Courreges, F., Smith-Guerin, N., Poisson, G.,Vieyres, P., Gourdon, A., Szpieg, M., and Merigeaux, O.: Real-time exhibition of a simulated space tele-echography using an ultra-light robot. In Proc. ISAIRAS, Canada (2001)
3. Eldridge, B., Gruben, K., LaRose, D., Funda, J., Gomory, S., Karidis, J., McVicker, G., Taylor, R., Anderson, J.: A Remote Center of Motion Robotic Arm for Computer Assisted Surgery. Robotica, 14(1), 103-109 (1996)
4. Essomba, T., Nouaille, L., Laribi, M. A., Nelson, C. A., Zeghloul, S., Poisson, G.: Spherical wrist dimensional synthesis adapted for tool-guidance medical robots. Mechanics and Industry, 15(3), 217-223 (2014)
5. Kang, H., Wen, J. T.: EndoBot : a robotic assistant in minimally invasive surgeries. In Proc. of the IEEE Intl. Conf. on Robotics and Automation, Seoul, South Korea, pp. 2031-2036 (2001)
6. Laribi, M. A., Rivière, T., Arsicault, M., and Zeghloul, S.: A design of slave surgical robot based on motion capture. Proc. 2012 IEEE International Conference on Robotics and Biomimetics (ROBIO2012), December 11-14, 2012, Guangzhou, China, pp. 600-605 (2012)
7. Nelson, C. A., Zhang, X.: Equivalent Mechanisms Techniques for Redesign of a Spherical Surgical Tool Manipulator. ASME IDETC 2010, Montréal, Québec, Canada, Aug. 15-18, 2010, ASME Paper No. DETC2010-28367 (2010)
8. Nouaille, L., Laribi, M. A., Nelson, C. A., Essomba, T., Poisson, G., Zeghloul, S.: Design Process for Robotic Medical Tool-Guidance Manipulators. Proc. IMechE Part C: J Mechanical Engineering Science, 230(2), 259-275 (2016)
9. Nouaille, L., Poisson, G., Zhang, X., Nelson, C. A.: Method of Dimensional Optimization of Spherical Robots for Medical Applications using Specialized Indices. Advanced Robotics, 28(3), 173-186 (2014)
10. Olds, K.: Global Indices for Kinematic and Force Transmission Performance in Parallel Robots. IEEE Transactions on Robotics, 31(2), 494-500 (2015)
11. Rininsland, H.: ARTEMIS. A telemanipulator for cardiac surgery. European Journal of Cardio-thoracic Surgery, 16(2), 106-111 (1999)
12. Rosen, J., Brown, J. D., Chang, L., Barreca, M., Sinanan, M., and Hannaford, B.: The Blue-DRAGON – a System for Measuring the Kinematics and the Dynamics of Minimally Invasive Surgical Tools In-Vivo. In Proc. IEEE International Conference on Robotics and Automation, Washington, DC, pp. 1876-1881 (2002)
13. Schinozuka, M.: Monte Carlo solution of structural dynamics, Computers and Structures 2: 855–874 (1972)
14. Tanev, T. K., Cammarata, A., Marano, D., Sinatra, R.: Elastostatic model of a new hybrid minimally invasive surgery robot. In Proc. 14th IFToMM World Congress, Taipei, Taiwan, October 25-30 (2015)
15. Vaida, C., Gherman, B., Pisla, D., Plitea, N.: A spherical robot arm for instruments positioning in minimally invasive medical applications. In Proc. 2nd IFToMM Asian Conference on Mechanism and Machine Science, Tokyo, Japan, November 7-10 (2012)
16. Zemiti, N., Ortmaier, T., Vitrani, M. A., Morel, G.: A force controlled laparoscopic surgical robot without distal force sensing. In Proc. 9th Int. Symp. on Experimental Robotics, ISER'04, Singapore (2004)
17. Zhang, X., and Nelson, C. A.: Multiple-Criteria Kinematic Optimization for the Design of Spherical Serial Mechanisms using Genetic Algorithms. Journal of Mechanical Design, 133(1), 011005 (2011)
18. Zhang, X., Nelson, C. A.: Kinematic Analysis and Optimization of a Novel Robot for Surgical Tool Manipulation. Journal of Medical Devices, 2(2), 021003 (2008)